Nephrol Dial Transplant (2012) 27: 2355–2364
doi: 10.1093/ndt/gfr649
Advance Access publication 6 December 2011

CHD1L: a new candidate gene for congenital anomalies of the kidneys and urinary tract (CAKUT)

Antje Brockschmidt[1,*], Boidinh Chung[1,*], Stefanie Weber[2], Dagmar-Christiane Fischer[3,4], Maria Kolatsi-Joannou[5], Laura Christ[1], André Heimbach[1,6], Diamant Shtiza[7], Günter Klaus[8], Giacomo D. Simonetti[9], Martin Konrad[10], Paul Winyard[5], Dieter Haffner[3], Franz Schaefer[2] and Ruthild G. Weber[1,6]

[1]Institute of Human Genetics, Rheinische Friedrich-Wilhelms-University, Bonn, Germany, [2]Division of Pediatric Nephrology, University Children's Hospital, University of Heidelberg, Heidelberg, Germany, [3]Department of Pediatric Kidney, Liver and Metabolic Diseases, Hannover Medical School, Hannover, Germany, [4]Department of Pediatrics, University Children's Hospital, Rostock, Germany, [5]Institute of Child Health, University College London, London, UK, [6]Department of Human Genetics, Hannover Medical School, Hannover, Germany, [7]Departamenti I Pediatrise Sherbimi I Nefrologjise, Qendra Spitalore Universitare 'Nene Tereza', Tirana, Albania, [8]KfH-Pediatric Kidney Center, Marburg, Germany, [9]Division of Pediatric Nephrology, University Children's Hospital, Bern, Switzerland and [10]Department of General Pediatrics, University Children's Hospital, Münster, Germany

Correspondence and offprint requests to: Ruthild G. Weber; E-mail: ruthild.weber@ukb.uni-bonn.de
*Both authors contributed equally to this work.

Abstract

Background. Recently, we identified a microduplication in chromosomal band 1q21.1 encompassing the *CHD1L/ALC1* gene encoding a chromatin-remodelling enzyme in congenital anomalies of the kidneys and urinary tract (CAKUT) patient.

Methods. To explore the role of *CHD1L* in CAKUT, we screened 85 CAKUT patients for mutations in the *CHD1L* gene and performed functional analyses of the three heterozygous missense variants detected. In addition, we quantitatively determined *CHD1L* expression in multiple human fetal and adult tissues and analysed expression of CHD1L protein in human embryonal, adult and hydronephrotic kidney sections.

Results. Two of three novel heterozygous missense variants identified in three patients were not found in >400 control chromosomes. All variants lead to amino acid substitutions in or near the CHD1L macro domain, a poly-

ADP-ribose (PAR)-binding module interacting with PAR polymerase 1 (PARP1), and showed decreased interaction with PARP1 by pull-down assay of transfected cell lysates. Quantitative messenger RNA analysis demonstrated high *CHD1L* expression in human fetal kidneys, and levels were four times higher than in adult kidneys. In the human embryo at 7–11 weeks gestation, CHD1L immunolocalized in the early ureteric bud and the S- and comma-shaped bodies, critical stages of kidney development. In normal postnatal sections, CHD1L was expressed in the cytoplasm of tubular cells in all tubule segments. CHD1L expression appeared higher in the hydronephrotic kidney of one patient with a hypofunctional *CHD1L* variant than in normal kidneys, recapitulating high fetal levels.

Conclusion. Our data suggest that *CHD1L* plays a role in kidney development and may be a new candidate gene for CAKUT.

Keywords: CAKUT; CHD1L; expression pattern; hypofunctional variant; kidney development

Introduction

Renal tract malformations can occur at the level of the kidney (e.g. aplasia, hypoplasia, dysplasia with and without cysts or duplex kidney), collecting system (e.g. hydronephrosis or hydroureter), bladder [e.g. vesicoureteral reflux (VUR)] or urethra (e.g. posterior urethral valves) and are subsumed by the term congenital anomalies of the kidneys and urinary tract (CAKUT). CAKUT comprise ~15% of all congenital anomalies detected prenatally and are found in >250 syndromes and in more than one-third of chromosome aberrations [1]. Among these are disorders like the chromosome 22q11.2 deletion and the 22q11.2 microduplication syndromes caused by microdeletion or microduplication of chromosomal region 22q11.2, suggesting that in certain genes both a loss-of-function and a gain-of-function may lead to CAKUT [2–4].

A number of developmental genes, such as *EYA1* and *SIX1* causing autosomal dominant (AD) branchio-oto-renal syndrome [5, 6], *HNF1B/TCF2* associated with AD renal cysts and diabetes syndrome [7], and *PAX2* causing AD renal-coloboma syndrome [8], have been implicated in the pathogenesis of CAKUT [9].

To screen for novel chromosomal regions and genes associated with CAKUT pathogenesis, we recently performed genome-wide array-based comparative genomic hybridisation in 30 children with various CAKUT phenotypes and extrarenal symptoms [10]. In a patient presenting with renal hypoplasia, proximal ureteric stenosis and additional anomalies, we detected a duplication of 2.73 Mb in 1q21.1 [10]. Among the genes duplicated was *CHD1L* (syn.: *ALC1*, *amplified in liver cancer 1*), which encodes the chromodomain helicase DNA-binding protein 1-like protein. CHD1L belongs to the Snf2 family of helicase-related ATP-hydrolyzing proteins and contains a helicase-like region, which is similar to that of other members of the Snf2-like group, such as Snf2, Iswi, Chd1 and CHD7 [11]. ATPases of this family often combine a helicase domain with motifs that mediate selective recognition of protein modifications. In CHD1L, this is a macro domain, which is an ADP-ribose/poly-ADP-ribose (PAR)-binding module [12]. *CHD1L* has been implicated as an oncogene with a major impact in hepatocellular carcinoma development [13–15] and has been identified as a chromatin-remodelling enzyme that interacts with PAR and catalyses PAR polymerase 1 (PARP1)-stimulated nucleosome sliding [16, 17].

Chromatin-remodelling and -modifying enzymes are predicted to play key roles in differentiation, development and tumour pathogenesis via effects on chromatin structure and accessibility [18, 19]. Mutations in *CHD7*, a gene structurally related to *CHD1L*, cause CHARGE syndrome, which includes renal developmental anomalies [20–22]. Therefore, in this study, we screened 85 CAKUT patients for mutations in the *CHD1L* gene and performed functional analyses of the three heterozygous missense variants identified. In addition, we quantitatively determined *CHD1L* expression in multiple human fetal and adult tissues and analysed expression of CHD1L protein in human embryonal, adult and hydronephrotic kidney sections. Our data provide evidence for a role of CHD1L in kidney development and for *CHD1L* mutations in the anomalies of the renal tract.

Materials and methods

Patients

The mutation analysis was approved by the ethics committee of the Medical Faculty of the University of Heidelberg, Germany, and informed assent and/or consent was obtained from the patients and/or parents as appropriate. Eighty-five patients presenting with different CAKUT phenotypes, defined by clinical and renal sonographic assessment, were screened for *CHD1L* mutations. The patients presented with one or more of the following CAKUT phenotypes: kidney agenesis (6 patients), kidney hypoplasia (17 patients), dysplastic kidneys (39 patients), medullary cystic kidney disease (3 patients) and duplex kidney (11 patients). Nine patients showed ureteral anomalies: proximal ureteral stenosis (1 patient) and megaureter/hydronephrosis (8 patients). Twenty-four patients presented with VUR. Posterior urethral valves were identified in eight patients. In three patients, heterozygous missense variants were detected in the *CHD1L* gene.

Patient 1. The boy was the first child of non-consanguineous healthy parents. Renal abnormalities are not known in the family. While the kidney ultrasound of the mother during pregnancy did not disclose any abnormality, the father was not available for examination by renal ultrasound. The antenatal story of the patient was uneventful, and prenatal ultrasound did not disclose any abnormality. The boy was born at term with weight (3750 g) and length (50 cm) within the normal range and without dysmorphic features. A febrile urinary tract infection (UTI) occurred at age 4 months, which led to the diagnosis of a hypodysplastic right kidney with right-sided grade III–IV and left-sided grade II VUR demonstrated by renal ultrasound and micturating cysto-urethrography (MCUG). While no further UTI occurred, growth of the right kidney was impaired. At the age of 6 years, the kidney was small for age (volume 34 mL, <3rd percentile), whereas the contralateral kidney showed compensatory hypertrophy (volume 100 mL, >97th percentile). Blood pressure and urine analysis were normal, in particular no leucocyturia or erythrocyturia, no glucosuria and no pathological protein excretion were detected. The child exhibited normal psychomotor and somatic development.

Patient 2. The boy is Albanian and was born in Kosovo after an uneventful pregnancy. The parents were unrelated and healthy with normal renal morphology on the ultrasound scan. During the first year of life, the patient developed repeated episodes of febrile UTI. Clinical workup revealed a severe CAKUT phenotype with bilateral massive hydronephrosis due to obstructive megaureters. He received bilateral pyelostomy at 18 months of age. The further clinical course was complicated by repeated UTIs leading to nephrectomy of the left kidney at age 2.5 years. The ureteropelvic drainage of the right kidney was switched to a cutaneous ureterostomy at the age of 5 years when the family moved to Germany. At that time, advanced chronic

renal failure [estimated glomerular filtration rate (GFR) 23 mL/min/1.73m^2], uraemic bone disease and growth failure (height 14 cm, <3rd percentile) were diagnosed. Further findings were unilateral cryptorchidism and subglottic stenosis, presumed secondary to repeated and prolonged mechanical ventilation. Renal failure gradually progressed and renal replacement therapy was initiated at the age of 13 years. Right-sided nephrectomy and excision of the hydroureter were performed at the time of renal transplantation at the age of 16 years. Histopathological workup showed atrophy of the renal parenchyma, chronic tubulointerstitial inflammation and chronic ureteritis.

Patient 3. The boy was referred for clinical examination at 3 weeks of age with severe renal insufficiency (estimated GFR 17 mL/min/1.73m^2). Ultrasound revealed bilateral hypodysplasia of the kidneys. No VUR was detected by MCUG. Extrarenal organ malformations were not observed. At the age of 12 months, cystoscopy revealed a posterior urethral valve with membranous stenosis of the urethra and a trabeculated bladder. The posterior urethral valve was subsequently excised. During the following 8 years, renal function declined to a GFR <10 mL/min/1.73m^2 and peritoneal dialysis was started at 9 years of age. At the age of 10 years, the patient received a cadaveric kidney transplant with immediate graft function.

Materials

All immunohistochemistry was performed on formalin-fixed paraffin-embedded sections. Samples included (i) phenotypically normal human kidney samples from chemically induced terminations of pregnancy between 7 and 11 weeks of gestation ($n = 7$), collected by the Wellcome Trust and Medical Research Council-funded Human Developmental Biology Resource at the UCL Institute of Child Health, London, UK. Informed consent to analyse these samples was obtained from the mothers involved, and use was approved by the Joint University College London/University College Hospital Committee on the Ethics of Human Research. (ii) Normal postnatal kidneys ($n = 4$) from autopsies of children who had died at a mean age of 3.5 years (range: 20 months to 8 years) from causes not associated with kidney disease, provided by the Department of Forensic Medicine of the University of Rostock, Germany. Use of these samples was approved by the ethics committee of the University of Rostock. (iii) Kidney and ureteric specimens from Patient 2, who was nephrectomized at time of transplantation, was provided by the Pathology Department of the University of Marburg, Germany.

Sequence analysis of CAKUT patients

Genomic DNA samples were obtained from peripheral blood of patients and blood donors (controls). Twenty-four primer pairs were designed to amplify 23 coding exons and all adjacent splice sites, the 5′-untranslated region (5′-UTR) and the 3′-untranslated region (3′-UTR) of the *CHD1L* gene by standard polymerase chain reaction (PCR). The entire coding region including the splice sites at the exon–intron boundaries and the 5′- and 3′-UTR was screened for mutations in 61 CAKUT patients by direct sequencing using the Big-Dye Terminator v1.1 Sequencing Kit (Applied Biosystems Deutschland GmbH, Darmstadt, Germany) and an automated capillary sequencer (ABI 3730; Applied Biosystems Deutschland GmbH). An additional 24 CAKUT patients were only screened for mutations in the *CHD1L* exons 18, 19 and 21, in which missense variants had been identified, because there was not enough DNA available to analyse the entire coding region. The effects of the detected missense variants were analysed with the web-based prediction programme PolyPhen (http://genetics.bwh.harvard.edu/pph/index.html). When available, parental DNA samples were specifically analysed for the variant found in their child. Primer sequences and PCR conditions are available upon request. Nucleotide numbering of the *CHD1L* variants reflects complementary DNA (cDNA) numbering in the GenBank reference sequence NM_004284, and +1 corresponds to the A of the ATG translation initiation codon.

Tissue-specific messenger RNA expression analysis

To test for tissue-specific expression of the *CHD1L* gene, we used the Human Multiple Tissue cDNA (MTC) Panels I and II and the Human Digestive System MTC panel for fetal tissues (Clontech—Takara Bio Europe, Saint Germain-en-Laye, France). In the MTC panels, fetal cDNAs were pooled from 13 to 59 spontaneously aborted Caucasian fetuses aged 16–37 weeks. Relative quantifications in real-time experiments were performed on the ABI Prism 7900HT Fast Real-Time PCR System (Applied Biosystems Deutschland GmbH) using the inventoried TaqMan Gene Expression Assay for the *CHD1L* gene (Applied Biosystems Deutschland GmbH). Each sample was normalized to the TaqMan Endogenous Control Beta-2-Microglobulin (Applied Biosystems Deutschland GmbH), and comparative C_t quantification [delta–delta ($\Delta\Delta$) C_t] was applied. The expression of the *CHD1L* gene in the other tissues was calculated relative to the expression in the fetal kidney, which was arbitrarily defined as 1. Each sample was assayed in triplicate.

Immunohistochemistry of renal sections

Immunohistochemical analysis of tissue samples (5 µm sections mounted on Superfrost® slides) was performed essentially as described previously [23, 24]. Briefly, sections were deparaffinized in histoclear or xylene and dehydrated through a series of graded alcohols prior to blocking endogenous peroxidase. For antigen retrieval, slides were boiled in 0.01 M citrate buffer (pH 6.0) using a microwave (1 × 10 min or 3 × 8 min, 450 W). Unspecific binding sites and endogenous biotin were saturated [10% fetal calf serum (FCS)/1% bovine serum albumin or 10% horse serum and avidin in phosphate-buffered saline (PBS); Vector Laboratories, Burlingame, CA; 20 min at room temperature] prior to incubation (4°C, over night) with the specific antibody [CHD1L, rabbit polyclonal IgG purchased from Atlas Antibodies (Catalog Number HPA 028 670; diluted 1:300 for postnatal and 1:500 for embryonal sections), Stockholm, Sweden; megalin (proximal tubule), rabbit polyclonal antiserum (1:100; Santa Cruz Biotechnology Inc., Heidelberg, Germany); Tamm–Horsfall protein (THP, thick ascending limb of Henle's loop and distal tubule), rabbit polyclonal antiserum (1:500; Santa Cruz Biotechnology); aquaporin-2 (collecting duct), rabbit polyclonal antiserum (1:100; Santa Cruz Biotechnology)]. Subsequently, slides were treated with a biotin-labelled secondary antibody (Vector Laboratories) prior to incubation with peroxidase-conjugated avidin–biotin complexes (Vectastain Elite ABC kit; Vector Laboratories) and 3,3′-diaminobenzidine (Merck KG, Darmstadt, Germany; tablets of 10 mg). Counterstaining was carried out with haematoxylin. Slides derived from renal cell carcinoma were used as positive controls for *CHD1L* expression. For negative controls, the specific antibody was replaced by an unrelated antibody of the same subclass (isotype control). Slides were examined with a Zeiss Axiophot II (Jena, Germany) or a Leica DMI 4000 microscope (Wetzlar, Germany) equipped with a digital camera (DFC 320 R2; Leica).

CHD1L expression constructs

The generation of the full-length human wild-type *CHD1L* expression construct has been described elsewhere, and this construct was kindly provided by Zuzana Horejsi and Simon J. Boulton from the DNA Damage Response Laboratory, Clare Hall, London Research Institute, South Mimms, EN6 3LD, UK [16].

The three identified missense variants, Gly700Arg (exon 18), Ile765Met (exon 19) and Ile827Val (exon 21), were introduced into wild-type *CHD1L* by PCR mutagenesis with primers (Metabion, Martinsried, Germany) containing the corresponding mutation (CHD1L-forward: 5′-GCCAAGAGAAGGAGACTCATAGAGG-3′, CHD1L-Gly700Arg-forward: 5′-CCAGAGGACCTTGAGAATAGGGAAGAGAGC-3′, CHD1L-Gly700Arg-reverse: 5′-GCTCTCTTCCCTATTCTCAAGGTCCTCTGG-3′, CHD1L-Ile765Met-forward: 5′-CGCTGAGCCAAGAAAAATGTATGAGCTGGC-3′, CHD1L-Ile765Met-reverse: 5′-GCCAGCTCATACATTTTTCTTGGCTCAGCG-3′, CHD1L-Ile827Val-forward: 5′-GAGGGCCTGAAGAAGGTATTTTTAGCAGC-3′, CHD1L-Ile827Val-reverse: 5′-GCTGCTAAAAATACCTTCTTCAGGCCCTC-3′, CHD1L-reverse: 5′-CCTACAGGTTGTCTTCCCAACTTGC-3′) and appropriate restriction enzymes for subcloning. Each amplicon was introduced as a 657-bp *Ppu*MI/*Xba*I (Fermentas Life Sciences, Burlington, Canada) restriction fragment into *Ppu*MI/*Xba*I digested wild-type *CHD1L* (untagged).

The myc-tagged full-length human wild-type *CHD1L* construct was generated by amplification of the provided untagged wild-type *CHD1L* plasmid with primers containing the appropriate restriction sites and lacking the stop codon (CHD1L_*Kpn*I_forward: 5′-GCTGACGGTACCGACATGGAGCGCGCGGGCGCT-3′, CHD1L_*Eco*RV_reverse: 5′-ctggatatcagcttctgctcAGGCACCAGCTGTCTTGAGGAGG-3′) and introduced as a 2.7-kb *Kpn*I/*Eco*RV restriction fragment into the eukaryotic expression vector pcDNA3.1/myc-His (Invitrogen by Life Technologies, Carlsbad, CA) containing a C-terminal myc and poly-His tag. The three missense variants, Gly700Arg, Ile765Met and Ile827Val, were amplified from the newly generated *CHD1L* constructs containing the corresponding variant with the primers CHD1L-forward: 5′-GCCAAGAGAAGGAGACTCATAGAGG-

3′ and CHD1L_*Eco*RV_reverse: 5′-ctggatatcagcttctgctcAGGCACCAGCT GTCTTGAGGAGG-3′ and in each case introduced as a 620-bp *Ppu*MI/*Eco*RV restriction fragment into the *Ppu*MI/*Eco*RV digested pcDNA3.1 wild-type *CHD1L* myc-tagged construct. All constructs were verified by sequencing.

Cell culture and transfection

Human embryonic kidney (HEK) 293T cells were grown in Dubecco's modified Eagle's medium (Gibco/Invitrogen) with 10% FCS and seeded 1 day prior to transfection. Cells were transiently transfected with 750 ng (100 μL Optimem, 2.5 μL Fugene) and 4 μg (400 μL Optimem, 12 μL Fugene) of myc-tagged wild-type and mutant *CHD1L* constructs, respectively, using Fugene® HD Transfection Reagent according to the manufacturer's instructions (Roche Diagnostics, Grenzach, Germany). Twenty-four hours after transfection, cells were lysed with 0.05 M HEPES supplemented with 1 mM dithiothreitol (DTT).

Immunoprecipitation of myc-tagged CHD1L proteins

For immunoprecipitation (IP) with anti-c-myc-conjugated agarose beads (Sigma Aldrich, St. Louis, MO), the ratio of protein lysate (in microgram) to anti-c-myc agarose (in microlitre) was 1:5. For each cell lysate, a suspension of anti-c-myc-conjugated agarose was settled in a microcentrifuge tube by a short spin (30 s at 8000 *g*), the supernatant was removed and the resin was washed three times with 150 μL 1× PBS. Subsequently, the respective cell lysate was added, and the final volume was brought to at least 200 μL with 1× PBS. The suspension of anti-c-myc agarose and cell lysate was incubated for 2.5 h on an orbital shaker at 4°C. Afterwards, the resin was pelleted by centrifugation and was washed twice with 150 μL 1× PBS. Finally, the supernatant was aspirated, except ~10 μL which were left above the agarose. For western blot analysis, 0.05 M HEPES buffer containing 1 mM DTT and 2× sodium dodecyl sulphate (SDS) sample buffer containing 400 mM DTT were added in a ratio of 1:1, and the samples were denatured for 5 min at 95°C.

Western blot analysis

Samples were used in equal amounts for SDS–polyacrylamide gel electrophoresis (SDS–PAGE; SE 600 Ruby; GE Healthcare, Freiburg, Germany). Proteins were blotted on a polyvinylidine difluoride membrane (Amersham Hybond-P; GE Healthcare) using a semi-dry transfer unit (TE77 ECL; GE Healthcare). The myc-tagged wild-type and mutant CHD1L proteins were detected using a mouse anti-c-myc monoclonal antibody (Santa Cruz Biotechnology Inc.), PARP1 using a rabbit anti-PARP1 polyclonal antibody (Abcam, Cambridge, UK) and β-actin using a rabbit anti-β-actin monoclonal antibody (Sigma Aldrich), each followed by incubation with horseradish peroxidase-conjugated goat anti-mouse or anti-rabbit antibodies (Santa Cruz Biotechnology Inc.). Blots were developed using a chemiluminescent detection kit (Applichem, Darmstadt, Germany). Western blot bands were quantified using the NIH ImageJ software.

Immunofluorescence

HEK 293T cells, which were transiently transfected with empty pcDNA3.1/myc-His expression vector (mock) or wild-type or mutant *CHD1L* constructs, were seeded on coverslips before fixation with 4% wt/vol paraformaldehyde, permeabilization with 0.1% Triton X-100 and blocking with 5% fat-free milk powder/0.1% Triton X-100/1% goat serum. CHD1L was detected via a primary rabbit anti-CHD1L polyclonal antibody (1:750; Atlas Antibodies) and a secondary goat anti-rabbit Alexa Fluor 568 labelled antibody (1:350; Invitrogen). Alexa Fluor 488 phalloidin (1:40; Invitrogen), which specifically detects F-actin, was used to visualise actin filaments within the cytoplasm. Nuclei were visualised with 4',6-diamidino-2-phenylindole counterstain. Fluorescent images were captured using a Leica DMRXA2 epifluorescence microscope.

Results

CHD1L mutation analysis in CAKUT patients

Sequencing of the entire coding region of the *CHD1L* gene in 61 CAKUT patients and of the *CHD1L* exons 18, 19 and 21 in 24 additional CAKUT patients revealed three different heterozygous missense variants. The variant found in Patient 1 (whose parents were not available for genetic testing) was a guanine-to-adenine transition at nucleotide position 2098 in exon 18 leading to a glycine-to-arginine substitution (c.2098G>A;p.Gly700Arg). The Gly700Arg variant was not found in 440 control chromosomes from central European individuals and was predicted to be probably damaging using the web-based PolyPhen software. The variant found in Albanian Patient 2 (inherited from his mother, who had no kidney or urinary tract anomalies on ultrasound) was an adenine-to-guanine transition at nucleotide position 2295 in exon 19 leading to an isoleucine-to-methionine substitution (c.2295A>G;p.Ile765Met). The Ile765Met variant was found in one of 430 control chromosomes from central European blood donors in whom a subtle CAKUT phenotype was not excluded, but not in 136 control chromosomes from Albanian individuals, and was predicted to be possibly damaging. The variant found in Patient 3 (inherited from his father, who was not available for examination by renal ultrasound) was an adenine-to-guanine transition at nucleotide position 2479 in exon 21 leading to an isoleucine-to-valine substitution (c.2479A>G;p.Ile827Val). The Ile827Val variant was not found in 402 control chromosomes from central European individuals and was predicted to be benign (Figure 1). All affected amino acids are conserved (p.Ile765) or highly conserved (p.Gly700 and p.Ile827) in higher animals.

CHD1L messenger RNA expression in different human tissues

To further investigate whether CHD1L is associated with the CAKUT phenotype, we quantified the messenger RNA (mRNA) levels of *CHD1L* in various fetal and adult tissues including the kidney (Figure 2). *CHD1L* was expressed in all analysed tissues. In the fetus, *CHD1L* expression was highest in brain followed by kidney and then by muscle, liver, thymus, lung, heart and spleen. Testis showed the highest *CHD1L* mRNA expression level of all adult tissues (data not shown). Fourfold less expression was measured in adult brain, followed by liver, muscle, pancreas, small intestine, ovary, kidney, colon, prostate, placenta, heart, lung, spleen and leukocytes. The *CHD1L* mRNA levels in fetal kidney were approximately four times higher than in adult kidney. Thus, among all corresponding fetal and adult tissues investigated, the fetal to adult expression ratio was highest in the human kidney.

Localization of the CHD1L protein in the normal human developing kidney

At 7 weeks gestation, the developing metanephric kidney consists of the central epithelial ureteric bud, with numerous peripheral branches that will give rise to the adult collecting ducts and collecting system and two types of mesenchyme: loose mesenchyme that will form stroma of the mature organ and condensing or condensed mesenchyme adjacent to the bud tips which undergoes mesenchymal-to-epithelial transformation to form the remainder of the nephrons from glomerulus to distal tubules. During the latter process, this 'induced' mesenchyme goes through vesicle, comma- and

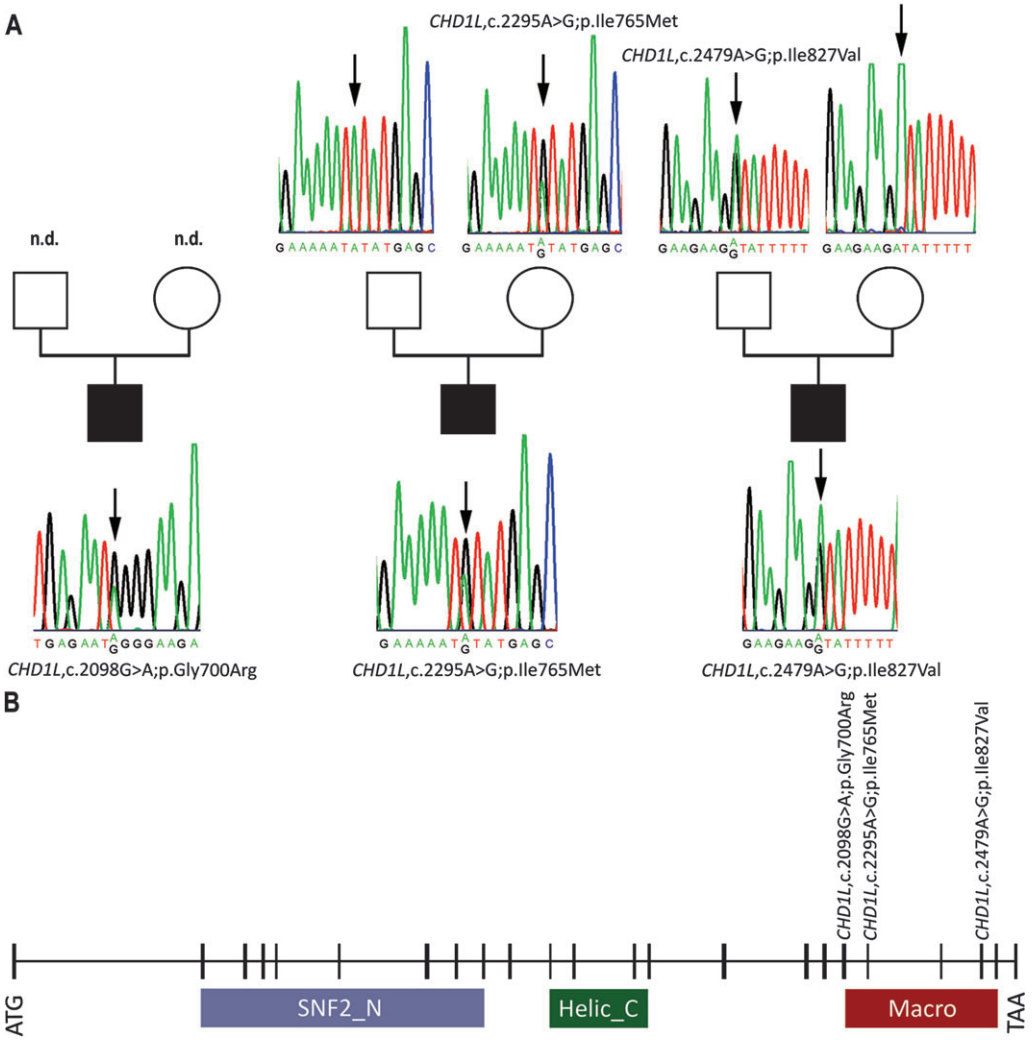

Fig. 1. Identification of *CHD1L* variants in CAKUT patients. Pedigrees and electropherograms of the three patients with the *CHD1L* missense variants: *CHD1L*,c.2098G>A;p.Gly700Arg (exon 18), *CHD1L*,c.2295A>G;p.Ile765Met (exon 19) and *CHD1L*,c.2479A>G;p.Ile827Val (exon 21). The affected nucleotide positions in the electropherograms are marked by arrows (**A**). Genomic location of the three missense variants within the *CHD1L* gene: *CHD1L*,c.2098G>A;p.Gly700Arg (exon 18), *CHD1L*,c.2295A>G;p.Ile765Met (exon 19) and *CHD1L*,c.2479A>G;p.Ile827Val (exon 21) relative to the functional Snf2 family N-terminal domain (SNF2_N), the helicase superfamily C-terminal domain (Helic_C) and the macro domain (Macro) of the CHD1L protein. Note that all variants are localized close to or within the macro domain (**B**).

S-shaped body stages before the first identifiable glomeruli and tubule segments can be discerned. The first site with identifiable CHD1L immunoreactivity was the ureteric bud, where protein was detected in rare cells in early cortical bud branches, although not in the more mature medullary segments. At later stages from 8 to 11 weeks, sporadic staining of individual cells was detected in loose mesenchyme, but strongly immunoreactive CHD1L was detected as mesenchyme condensed, with clear expression in early nephron precursors. Occasional positive cells were still detected in the ureteric bud, predominantly in the outer cortex where the bud was in intimate contact with the condensing mesenchyme. Subcellular localization was mainly nuclear, although a cytoplasmic signal could not be ruled out in some cells. Positive cells were also observed in some more mature structures, such as fully formed glomeruli or tubular structures (Figure 3). By immunofluorescence, CHD1L was exclusively localized to the nucleus of HEK cells (Figure 3). The subcellular localization of mutant CHD1L in HEK cells transfected with constructs expressing variant *CHD1L* was nuclear and thus not different from endogenous CHD1L or after wild-type *CHD1L* transfection (data not shown).

Localization of the CHD1L protein in the normal human postnatal kidney

In the normal kidney from a 5-year-old boy (autopsy material), CHD1L was immunolocalized to tubular cells in all segments of the tubule system. This was verified by staining of parallel sections with established markers of the tubular system, i.e. megalin for the proximal tubule, THP for the Henle loop and aquaporin-2 for the distal tubule and collecting duct. CHD1L staining was mainly detected in the cytoplasm and to a lesser extent in the nuclei of normal tubule cells (Figure 4).

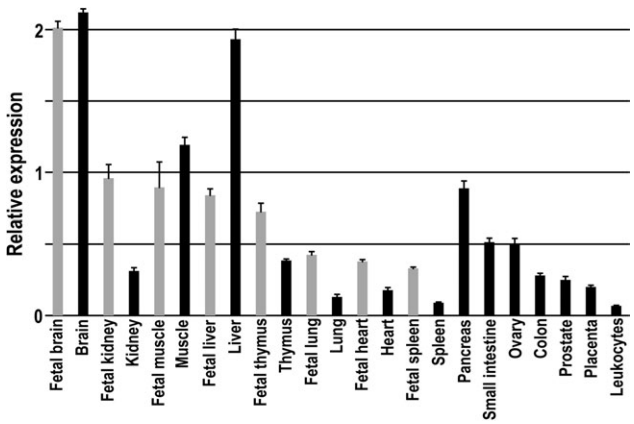

Fig. 2. Quantitative expression of *CHD1L* mRNA in human fetal and adult tissues. Expression levels were determined by real-time reverse transcription–PCR, normalized to *beta-2-microglobulin* mRNA expression and displayed relative to the *CHD1L* mRNA expression in the fetal kidney. *CHD1L* mRNA expression was the second highest in the fetal kidney compared to the other fetal tissues analysed and was four times as high in fetal compared to adult kidneys. Testis showed the highest *CHD1L* mRNA expression level of all adult tissues (data not shown).

CHD1L protein expression in the kidney and hydroureter from Patient 2

In the hydronephrotic kidney removed from Patient 2 at age 16 years prior to transplantation (nephrectomy material), CHD1L was also immunolocalized to tubular cells throughout the nephron. Although Patient 2 was older at nephrectomy than our healthy control, the intensity of CHD1L staining in the tubules appeared to be higher in the hydronephrotic kidney compared to the normal kidney. CHD1L staining was preferentially nuclear in the hydronephrotic kidney and in the corresponding hydroureter, where nuclear CHD1L expression was seen throughout the urothelium (Figure 4).

Interaction of mutant CHD1L protein with PARP1

To elucidate the functional effect of the three CHD1L variants with respect to their interaction with PARP1, we transfected HEK293T cells with c-myc-tagged wild-type and mutant *CHD1L* constructs. After cell lysis, IP of c-myc-tagged CHD1L protein was performed with anti-c-myc-conjugated agarose beads, followed by protein separation using SDS–PAGE. Western blot analysis with an anti-β-actin antibody demonstrated successful IP: β-actin signals were detectable in the input but not after IP (data not shown). PARP1 was immunoprecipitated together with CHD1L wild-type and mutant proteins and detected with an anti-PARP1-antibody, while immunoprecipitated c-myc-tagged wild-type and mutant CHD1L was detected with an anti-c-myc antibody. Visual inspection of western blot bands after IP showed that the signals for PARP1 in relation to the c-myc signals were clearly decreased in all mutants compared to wild-type CHD1L (Figure 5A).

Western blot bands were quantified using the NIH ImageJ software. The PARP1 and the respective c-myc Western blot signals after IP were measured, and the ratio of both signals was calculated to compare the interaction of PARP1 with wild-type and mutant CHD1L (Figure 5B). When averaging the results from three independent experiments, CHD1L and PARP1 interaction was diminished ~1.9-fold in variant Gly700Arg, ~2.3-fold in variant Ile765Met and ~2.2-fold in variant Ile827Val as compared to wild-type CHD1L.

Discussion

In this study, we describe heterozygous missense variants in the *CHD1L* gene in three male patients with a CAKUT phenotype characterized by uni- or bilateral hypodysplastic kidneys or hydronephrosis due to obstructive megaureters. Both patients with bilateral CAKUT had severe kidney failure requiring renal replacement therapy from age 9 or 13 years, respectively. The patient with unilateral hypodysplasia had a compensatory hypertrophy of the other kidney so that renal function was normal when he was last examined at 6 years of age. Two of the three variants in *CHD1L* were inherited from a parent, one of whom had a normal renal tract on ultrasound and the other being unavailable for sonographic examination. The parents of the third patient were not available for genetic testing, so inheritance or *de novo* occurrence could not be ascertained. Reduced penetrance and variable expressivity are not unusual in CAKUT; aberrations in the *PAX2*, *EYA1*, *SIX1* and *HNF1B/TCF2* genes cause highly variable and even missing renal phenotypes [9, 25].

There are various lines of evidence suggesting that the detected missense variants in *CHD1L* could be associated with the CAKUT phenotype in the patients of the present study. Firstly, two variants were not detected in at least 400 control chromosomes indicating a frequency of much <1% of these variants in the general population. The Albanian patient's missense variant was not found in 136 control chromosomes from Albanians, but in 1 of 430 control chromosomes from central Europeans, in whom a subtle CAKUT phenotype cannot be excluded because renal ultrasound was not routinely performed. Secondly, using the web-based PolyPhen software, two of the three variants were predicted to be probably or possibly damaging, while only one of the variants was predicted to be benign. This software tool predicts the possible impact of an amino acid substitution on the structure and function of a human protein using physical and comparative considerations but does not invariably have to be correct.

Further evidence for a role of CHD1L in kidney development came from quantitative mRNA analysis. The *CHD1L* gene was strongly expressed in the fetal human kidney, and the renal fetal to adult expression ratio (4:1) was highest compared to all other tissues tested, suggesting that *CHD1L* expression is of particular importance in the developing kidney. By immunohistochemistry of human embryonal sections with a CHD1L-specific antibody, we demonstrated that CHD1L immunolocalized in the early ureteric bud and in early nephron precursors from 7 through 11 weeks of gestation. For normal kidney development, mutual induction from the tips of the ureteric bud to the adjacent metanephric mesenchyme is essential, the sites in which CHD1L immunoreactivity was strongest. The bud lineage develops into the collecting system while induced mesenchyme undergoes comma- and S-shaped body morphological stages *en route* to forming the nephrons from glomerulus to distal tubule [26, 27]. The fact that CHD1L is expressed in both the

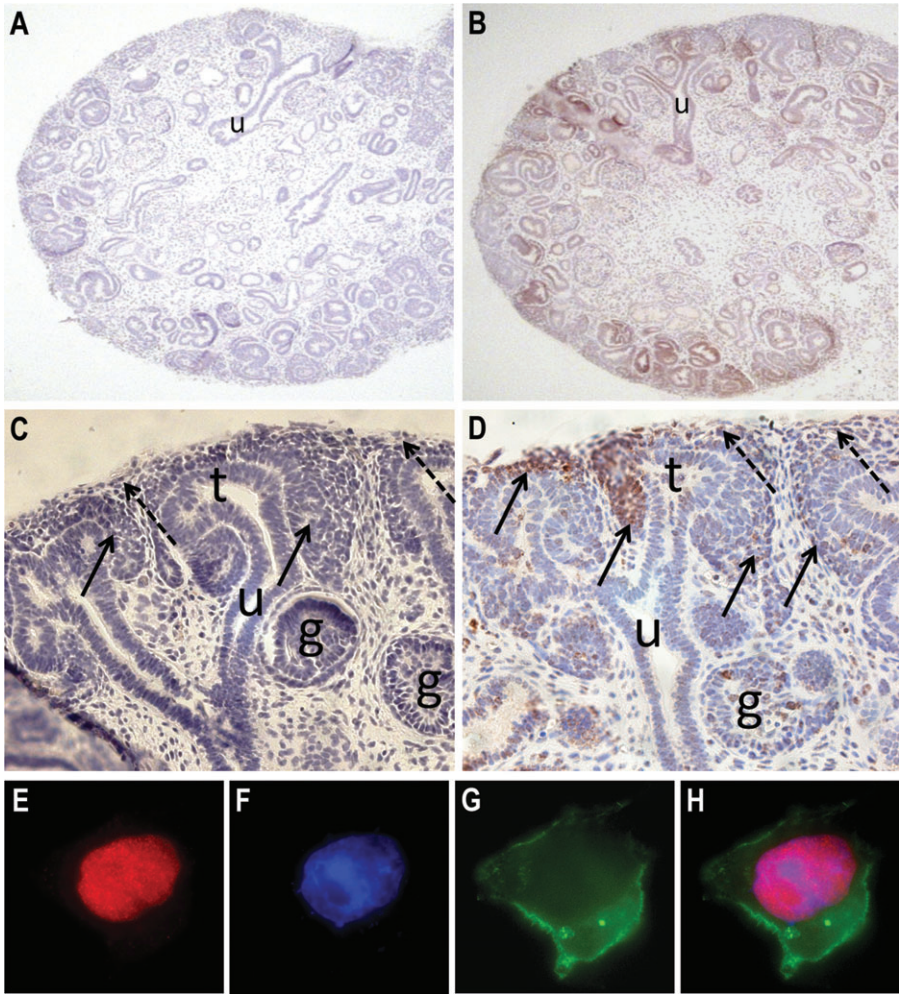

Fig. 3. Expression of CHD1L in developing human kidneys. Immunohistochemistry for CHD1L in 8–11 weeks human embryonal kidneys (**A**–**D**). All sections were counterstained with haematoxylin; positive immunohistochemical signal is brown; in control samples, 10% FCS was substituted for the primary antibody. Control panel from 8-week-old embryo demonstrating lack of background staining and illustrating early renal development with ureteric bud (u) and stages of nephron formation from comma shaped bodies through developing glomeruli (A). Nearby section demonstrating positive nuclear staining in the nephrogenic zone around the periphery of the kidney, where new nephrons are being formed (B). Control higher power view from 11 weeks showing ureteric bud, ureteric bud tip (t) and developing glomeruli (g), with loose mesenchyme (dotted arrow) and condensed mesenchyme (solid arrow) (C). Nuclear CHD1L was predominantly detected in condensed mesenchyme, although occasional positive cells were detected at the very tips of the ureteric bud (i.e. adjacent to the condensing mesenchyme) and in loose mesenchyme; fully formed glomeruli and deeper, more mature tubule segments were negative (not shown) (D). Immunofluorescence for CHD1L in HEK cells (**E**–**H**). CHD1L was stained for using a primary rabbit anti-CHD1L polyclonal antibody and a secondary goat anti-rabbit Alexa Fluor 568 labelled antibody (E), 4',6-diamidino-2-phenylindole was used as counterstain to delineate the nucleus (F), filamentous actin was visualized in the cytoplasm and at the cell membrane using Alexa488-phalloidin (G). The merged image clearly demonstrates the nuclear localization of CHD1L in embryonal cells (H).

ureteric bud and the metanephric mesenchyme may explain the different CAKUT phenotypes observed in patients with *CHD1L* variants, i.e. hydronephrosis secondary to obstructive megaureters, a malformation primarily of the ureter, and renal hypodysplasia, an anomaly primarily of the nephron.

While in human embryonal kidney cells, CHD1L was mainly detectable in the nucleus, in the kidneys from a 5-year-old child, CHD1L immunolocalized preferentially in the cytoplasm and only rarely to the nuclei of tubular cells in all parts of the mesenchyme-derived nephron. Interestingly, in the tubular cells and urothelium of the hydronephrotic kidney and hydroureter removed at the age of 16 years from Patient 2, the *CHD1L* expression seemed to be higher than in the normal kidney of the younger child recapitulating fetal levels, compatible with a lack of terminal nephron differentiation described in CAKUT. In the developing human kidney and the malformed kidney and ureter, *CHD1L* expression was predominantly nuclear, in line with recent reports that CHD1L is a chromatin-remodelling enzyme that catalyses nucleosome sliding and can act as a DNA damage response protein rapidly recruited to DNA damage sites in the nucleus [16, 17]. Chromatin remodelling is required for normal development in mammalian cells to orchestrate spatiotemporally distinct gene expression programmes necessary for cellular differentiation [18, 19]. Thus, the *CHD1L* variants identified here may induce deficits in differentiation in tubular cells of the kidney and in the urothelium due to impaired chromatin remodelling.

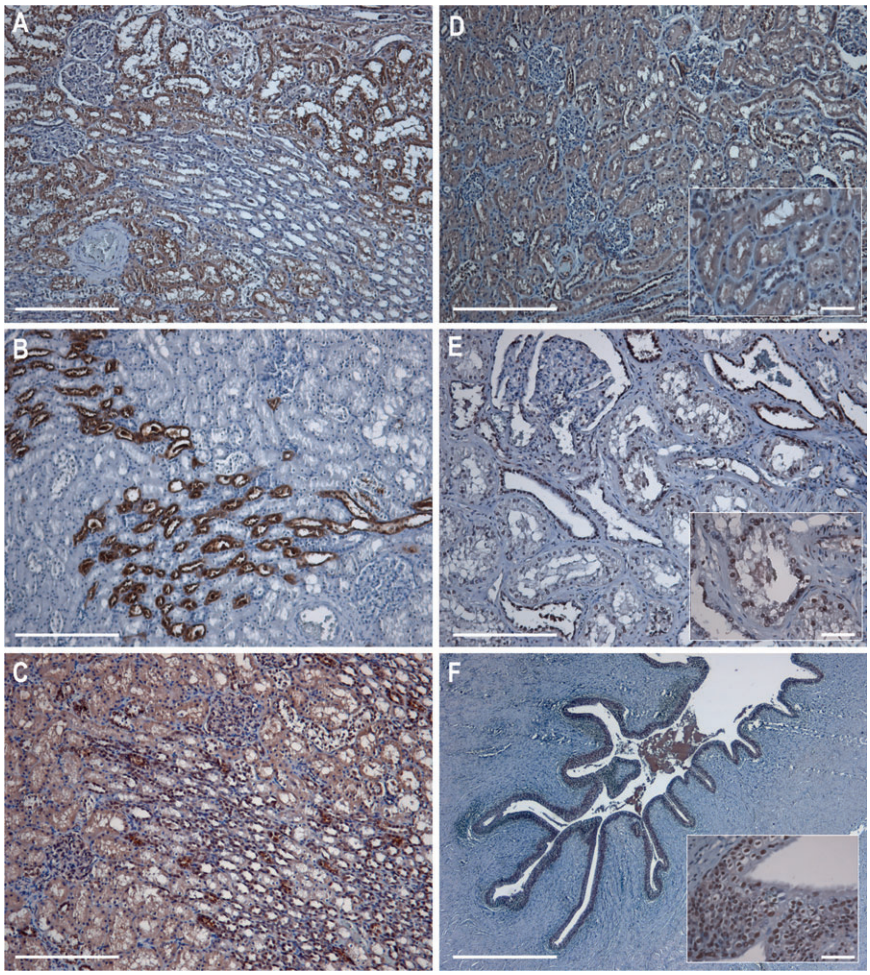

Fig. 4. Detection of megalin, THP and aquaporin-2 in normal human postnatal kidney (left panel) and of CHD1L in healthy and diseased specimens (right panel). Sections were probed with mAbs specific for megalin (**A**), THP (**B**), aquaporin-2 (**C**) and CHD1L (**D**–**F**) [normal kidney of 5-year-old (D); hydronephrotic kidney of 16-year-old Patient 2 with hypofunctional *CHD1L* variant (E); hydroureter from same patient (F)]. Bound antibody was visualized using biotin-labelled secondary antibody in combination with peroxidase-conjugated avidin–biotin complex and 3,3′-diaminobenzidine as substrate. Magnification: ×100 (bar: 200 μm) (A–E), ×25 (bar: 1 mm) (F) and ×400 (bar: 50 μm) (inserts in D–F). In normal postnatal sections, CHD1L was expressed in the cytoplasm of tubuloepithelial cells in all segments of the tubule system. CHD1L expression appeared higher in the dysplastic tubules of Patient 2 with a hypofunctional *CHD1L* variant than in normal kidneys, recapitulating high fetal levels, and was predominantly nuclear in tubular cells and urothelium of hydronephrotic kidney and hydroureter.

Impaired chromatin remodelling could alter the expression of key factors in renal system development such as glial-derived neurotrophic factor (GDNF), which is secreted by the metanephric mesenchyme and mediates ureteric bud induction from the nephric duct, and the RET receptor tyrosine kinase expressed in the ureteric bud to induce branching [28, 29]. In particular, the transcriptional fine tuning of factors regulating GDNF levels and spatial expression [30, 31] and the factors regulating RET [32–34] could be compromised by impaired chromatin remodelling due to mutated *CHD1L*. The dysregulated expression of the genes important for renal system development could cause aberrant interactions between the ureteric bud and the metanephric mesenchyme, which is known to cause renal hypodysplasia [27].

Strong evidence that mutations in a chromatin-remodelling enzyme can play a role in human renal tract anomalies comes from the *CHD7* gene, an ATP-dependent chromatin remodeller with structural homologies to *CHD1L* [11]. Mutations in *CHD7* cause CHARGE syndrome [20], which is associated with renal tract anomalies, such as horseshoe kidneys, renal agenesis, VUR and renal cysts, in ~20% of patients carrying *CHD7* mutations [22]. Likewise, in an animal model, a heterozygous mutation in Chd2, another member of the Snf2-like group of ATPases that function in chromatin remodelling, results in a complex renal phenotype consisting of glomerulopathy, proteinuria and significantly impaired kidney function in ~85% of mice [35, 36].

The hypothesis that the *CHD1L* mutations identified in CAKUT patients may impair chromatin remodelling is further substantiated by the fact that all variants resulted in amino acid substitutions within or close to the macro domain of the CHD1L protein. The intact C-terminal macro domain binds PAR and interacts with chromatin-associated PARP1 *in vitro* [16, 17]. PARP1 localizes to a large fraction of active promoters with a distinct role in determining gene expression [37] and strongly activates CHD1L ATPase- and chromatin-remodelling activities [17]. By pull-down assay of transfected cell lysates, we

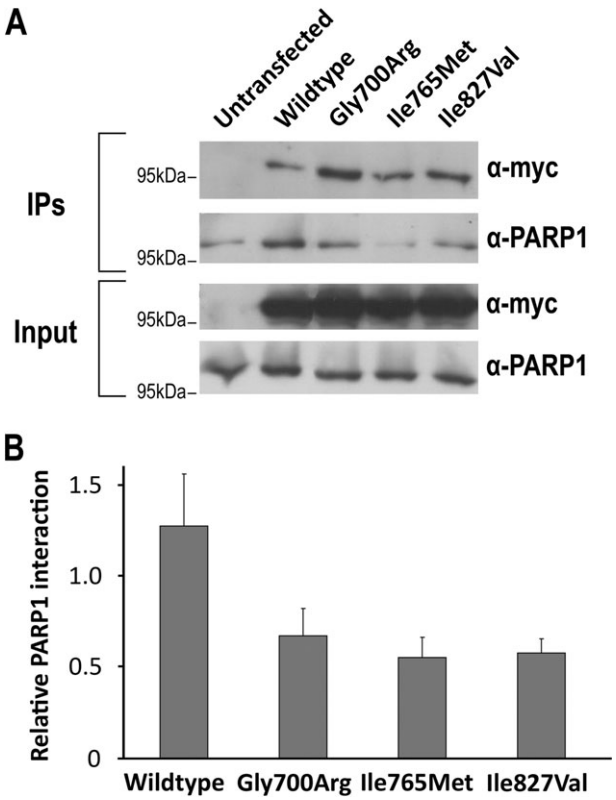

Fig. 5. Impairment of mutant CHD1L interaction with PARP1. Untransfected, wild-type and mutant CHD1L (Gly700Arg, Ile765Met and Ile827Val) transfected HEK293T cell lysates before (lower two rows) and after IP with c-myc-conjugated agarose beads (upper two rows), probed with anti-c-myc or anti-PARP1 antibodies, respectively (**A**). Bands detected after IP were quantified using the NIH ImageJ software. The signals measured for the co-precipitated PARP1 were divided by the signals for the immunoprecipitated CHD1L wild-type and mutant proteins. Results are means ± SEM for three independent experiments. CHD1L and PARP1 interaction is diminished in all three variants (Gly700Arg, Ile765Met and Ile827Val) (**B**).

found that all three CHD1L variants detected in our CAKUT patients showed decreased PARP1 interaction compared to wild-type CHD1L. These data suggest that the *CHD1L* variants identified may be hypofunctional and that the reduced interaction with PARP1 may compromise CHD1L ATPase- and chromatin-remodelling activities. This has recently been shown for *CHD1L* mutants in which the macro domain was deleted and for the specific macro domain Asp723Ala mutant [16, 17]. Interestingly, in this mutant, the amino acid substitution is located in the N-terminal part of the macro domain between Gly700Arg and Ile765Met, two variants identified here. The *CHD1L* macro domain deletion mutants and the Asp723Ala mutant showed no or decreased interaction with PAR and PARP1, and the recruitment of the Asp723Ala mutant to DNA damage sites was severely impaired, indicating at least a partial loss of function when the macro domain is deleted or altered at certain residues [16, 17]. If interaction with PARP1 is decreased like in the variants detected here, this functional deficit should have an impact on the ATPase- and chromatin-remodelling activities of CHD1L because they are strongly stimulated by PARP1 [16].

Conclusion

In summary, our study provides evidence that the ATP-dependent chromatin-remodelling enzyme CHD1L may play a role in renal development and in congenital anomalies of the kidneys and the urinary tract when altered. These conclusions are based on the following novel findings: (i) *CHD1L* expression was high in fetal kidneys and was four times higher in fetal compared to adult kidney. (ii) CHD1L immunolocalized in the early ureteric bud and early nephron precursors, critical stages of kidney development, in which CHD1L expression was predominantly nuclear and in the cytoplasm of tubule cells in the normal postnatal kidney. (iii) Heterozygous missense variants in *CHD1L* were detected in 3 of 85 CAKUT patients analysed, all leading to amino acid substitutions within or near the macro domain necessary for interaction with PAR and PARP1. (iv) Mutant CHD1L was hypofunctional with respect to interaction with PARP1. (v) The hydronephrotic kidney from a 16-year-old CAKUT patient with a hypofunctional *CHD1L* variant showed high nuclear CHD1L expression in dysplastic tubule cells mimicking the embryonal situation, compatible with a lack of terminal nephron differentiation described in CAKUT.

Acknowledgements. We express our gratitude to the children and their families for kindly participating in this study. We thank Dr Elke Wühl, Heidelberg, Germany and Dr M. Schröder, Frankfurt, Germany for providing patient data, Prof. Dr Roland Moll, Marburg, Germany and Dr Ulrich Hammer, Rostock, Germany for providing tissue samples and gratefully acknowledge embryonal samples supplied by the MRC/Wellcome-funded Human Developmental Biology Resource at the UCL Institute of Child Health, London, UK. Support for this study was obtained from the Else Kröner-Fresenius-Stiftung (2010_A97). M.K.-J. and P.W. were supported by grant funding from Kidney Research UK and Kids Kidney Research.

Conflict of interest statement. None declared.

References

1. Kerecuk L, Schreuder MF, Woolf AS. Renal tract malformations: perspectives for nephrologists. *Nat Clin Pract Nephrol* 2008; 4: 312–325
2. Ensenauer RE, Adeyinka A, Flynn HC *et al.* Microduplication 22q11.2, an emerging syndrome: clinical, cytogenetic, and molecular analysis of thirteen patients. *Am J Hum Genet* 2003; 73: 1027–1040
3. Shprintzen RJ. Velo-cardio-facial syndrome: 30 years of study. *Dev Disabil Res Rev* 2008; 14: 3–10
4. Portnoï MF. Microduplication 22q11.2: a new chromosomal syndrome. *Eur J Med Genet* 2009; 52: 88–93
5. Abdelhak S, Kalatzis V, Heilig R *et al.* A human homologue of the Drosophila eyes absent gene underlies branchio-oto-renal (BOR) syndrome and identifies a novel gene family. *Nat Genet* 1997; 15: 157–164
6. Ruf RG, Xu PX, Silvius D *et al.* SIX1 mutations cause branchio-oto-renal syndrome by disruption of EYA1-SIX1-DNA complexes. *Proc Natl Acad Sci U S A* 2004; 101: 8090–8095
7. Bingham C, Bulman MP, Ellard S *et al.* Mutations in the hepatocyte nuclear factor-1-beta gene are associated with familial hypoplastic glomerulocystic kidney disease. *Am J Hum Genet* 2001; 68: 219–224
8. Sanyanusin P, Schimmenti LA, McNoe LA *et al.* Mutation of the PAX2 gene in a family with optic nerve colobomas, renal anomalies and vesicoureteral reflux. *Nat Genet* 1995; 9: 358–364
9. Weber S, Moriniere V, Knüppel T *et al.* Prevalence of mutations in renal developmental genes in children with renal hypodysplasia: results of the ESCAPE study. *J Am Soc Nephrol* 2006; 17: 2864–2870

10. Weber S, Landwehr C, Renkert M *et al.* Mapping candidate regions and genes for congenital anomalies of the kidneys and urinary tract (CAKUT) by array-based comparative genomic hybridization. *Nephrol Dial Transplant* 2011; 26: 136–143
11. Flaus A, Martin DM, Barton GJ *et al.* Identification of multiple distinct Snf2 subfamilies with conserved structural motifs. *Nucleic Acids Res* 2006; 34: 2887–2905
12. Karras GI, Kustatscher G, Buhecha HR *et al.* The macro domain is an ADP-ribose binding module. *EMBO J* 2005; 24: 1911–1920
13. Ma NF, Hu L, Fung JM *et al.* Isolation and characterization of a novel oncogene, amplified in liver cancer 1, within a commonly amplified region at 1q21 in hepatocellular carcinoma. *Hepatology* 2008; 47: 503–510
14. Chen L, Hu L, Chan TH *et al.* Chromodomain helicase/adenosine triphosphatase DNA binding protein 1-like (CHD1l) gene suppresses the nucleus-to-mitochondria translocation of nur77 to sustain hepatocellular carcinoma cell survival. *Hepatology* 2009; 50: 122–129
15. Chen M, Huang JD, Hu L *et al.* Transgenic CHD1L expression in mouse induces spontaneous tumors. *PLoS One* 2009; 24: e6727
16. Ahel D, Horejsí Z, Wiechens N *et al.* Poly(ADP-ribose)-dependent regulation of DNA repair by the chromatin remodeling enzyme ALC1. *Science* 2009; 325: 1240–1243
17. Gottschalk AJ, Timinszky G, Kong SE *et al.* Poly(ADP-ribosyl)ation directs recruitment and activation of an ATP-dependent chromatin remodeler. *Proc Natl Acad Sci U S A* 2009; 106: 13770–13774
18. de la Serna IL, Ohkawa Y, Imbalzano AN. Chromatin remodelling in mammalian differentiation: lessons from ATP-dependent remodellers. *Nat Rev Genet* 2006; 7: 461–473
19. Ko M, Sohn DH, Chung H *et al.* Chromatin remodeling, development and disease. *Mutat Res* 2008; 647: 59–67
20. Vissers LE, van Ravenswaaij CM, Admiraal R *et al.* Mutations in a new member of the chromodomain gene family cause CHARGE syndrome. *Nat Genet* 2004; 36: 955–957
21. Lalani SR, Safiullah AM, Fernbach SD *et al.* Spectrum of CHD7 mutations in 110 individuals with CHARGE syndrome and genotype-phenotype correlation. *Am J Hum Genet* 2006; 78: 303–314
22. Jongmans MC, Admiraal RJ, van der Donk KP *et al.* CHARGE syndrome: the phenotypic spectrum of mutations in the CHD7 gene. *J Med Genet* 2006; 43: 306–314
23. Weber S, Taylor JC, Winyard P *et al.* SIX2 and BMP4 mutations associate with anomalous kidney development. *J Am Soc Nephrol* 2008; 19: 891–903
24. Fischer DC, Jacoby U, Pape L *et al.* Activation of the AKT/mTOR pathway in autosomal recessive polycystic kidney disease (ARPKD). *Nephrol Dial Transplant* 2009; 24: 1819–1827
25. Bellanné-Chantelot C, Chauveau D, Gautier JF *et al.* Clinical spectrum associated with hepatocyte nuclear factor-1beta mutations. *Ann Intern Med* 2004; 140: 510–517
26. Winyard P, Chitty LS. Dysplastic kidneys. *Semin Fetal Neonatal Med* 2008; 13: 142–151
27. Song R, Yosypiv IV. Genetics of congenital anomalies of the kidney and urinary tract. *Pediatr Nephrol* 2011; 26: 353–364
28. Schuchardt A, D'Agati V, Larsson-Blomberg L *et al.* Defects in the kidney and enteric nervous system of mice lacking the tyrosine kinase receptor Ret. *Nature* 1994; 367: 380–383
29. Chi X, Michos O, Shakya R *et al.* Ret-dependent cell rearrangements in the Wolffian duct epithelium initiate ureteric bud morphogenesis. *Dev Cell* 2009; 17: 199–209
30. Costantini F. Renal branching morphogenesis: concepts, questions, and recent advances. *Differentiation* 2006; 74: 402–421
31. Dressler GR. Advances in early kidney specification, development and patterning. *Development* 2009; 136: 3863–3874
32. Moreau E, Vilar J, Lelièvre-Pégorier M *et al.* Regulation of c-ret expression by retinoic acid in rat metanephros: implication in nephron mass control. *Am J Physiol* 1998; 275: F938–F945
33. Basson MA, Watson-Johnson J, Shakya R *et al.* Branching morphogenesis of the ureteric epithelium during kidney development is coordinated by the opposing functions of GDNF and Sprouty1. *Dev Biol* 2006; 299: 466–477
34. Clarke JC, Patel SR, Raymond RM Jr *et al.* Regulation of c-Ret in the developing kidney is responsive to Pax2 gene dosage. *Hum Mol Genet* 2006; 15: 3420–3428
35. Marfella CG, Ohkawa Y, Coles AH *et al.* Mutation of the SNF2 family member Chd2 affects mouse development and survival. *J Cell Physiol* 2006; 209: 162–171
36. Marfella CG, Henninger N, LeBlanc SE *et al.* A mutation in the mouse Chd2 chromatin remodeling enzyme results in a complex renal phenotype. *Kidney Blood Press Res* 2008; 31: 421–432
37. Krishnakumar R, Gamble MJ, Frizzell KM *et al.* Reciprocal binding of PARP-1 and histone H1 at promoters specifies transcriptional outcomes. *Science* 2008; 319: 819–821

Received for publication: 4.2.11; Accepted in revised form: 6.10.11